ARMD Seedling Fund – Phase I Final Technical Report

Enabling Electric Aviation with Ultra High Energy Lithium Metal Anode Batteries

John Lawson-PI (ARC-TSM), Thomas Miller (GRC-RPC0), James Wu (GRC-RPC0), William Bennett (GRC-RPC0), Charles Bauschlicher (ARC-TS), Justin Haskins (ARC-USRA), Brianne Scheidegger(GRC-RPC0)

Introduction

Green aviation's goals of high energy efficiency, low emissions and reduced noise can be achieved with electric aircraft. A principal barrier to electric aviation is high capacity energy storage. Li-ion batteries (LIB) with metal oxide cathodes, graphite anodes, and organic liquid electrolytes represent the state-of-the-art. However, LIBs have issues in terms of safety and thermal stability. In addition, LIBs fall short of meeting the power and energy requirements for electric aircraft [1]. Breakthroughs beyond the current state-of-the-art in battery technology are necessary to fully realize green aviation.

New electrode materials can provide the breakthroughs required to reach the next level in battery technology. Li metal anodes combined with advanced cathode materials such as Li-Air or Li-Sulfur offer substantial weight reduction and the promise of 5X improvements in specific energies, e.g. 1000 Wh/kg (Li-Air) compared to 200 Wh/kg for LIB [2]. The *fundamental* obstacle to the use of Li metal anodes in advanced, rechargeable, high energy batteries is poor charge/discharge cycling efficiency and safety concerns due to dendrite formation at the anode-electrolyte interface which can cause internal short circuits. Alternative electrolytes based on non-flammable, thermally and electrochemically stable ionic liquids (mixtures of cation and anion molecules) have the potential to solve these problems. For example, recent work has shown certain ionic liquids (IL) electrolytes may suppress the formation of dendrites and show improved cycling capabilities relative to traditional organic electrolytes [3]. The number of possible ionic liquids and other similar electrolytes is vast, and while some ILs show dendrite suppression, others do not. Identifying the fundamental factors controlling the performance of these ultra-high energy Lithium metal batteries (LMB) as well as developing tools for rapid screening and selection of optimal components for fabrication is required to assess fully their potential.

The global objective of this Seedling project is to develop an integrated experimental/computational infrastructure to accelerate fundamental understanding, screening and design of novel IL electrolytes for advanced ultra-high energy LMBs. The novelty of our approach results from the combination of validated computational modeling with experimental screening to produce a reliable predictive capability for the selection of optimal components, their fabrication parameters, and the design of ultra-high energy LMB that can meet energy storage challenges of current and future NASA missions and many terrestrial transportation application such as electric vehicles and aircraft.

In Phase I, LMBs with two different IL electrolytes were considered: [pyr14][TSFI] [4] which has shown significant dendrite suppression and Li anode cycling ability on the order of 1000 cycles in laboratory systems and [EMIM][BF_4] [5] which has shown little or no dendrite suppression and very poor cycle life [6]. Note that pyr14 and EMIM are cations and TSFI and BF_4 are anions. Chemical structures are shown in Figure 1.

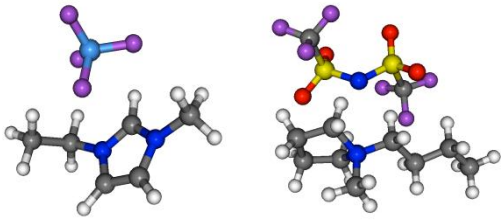

Figure 1 Chemical structure for ionic pairs of [EMIM][BF4] (left) and [pyr14][TSFI] (right)

For these two cases, we considered the following four essential elements. First, we determined properties of isolated ILs important for battery operation and found good agreement between simulation and experiment. Second, we made predictions about the structure and properties of the IL in the presence of an electrode; interaction of the ILs with the anode surface affects the local molecular ordering of the IL as well as its properties. Third, we considered chemical reactions between the IL electrolyte and the Li metal anode surface at zero applied voltage. Fourth, we built and characterized the performance of laboratory LMBs using the two ILs. Strong correlations were found between computations and experimental battery characterizations.

Approach

We performed an integrated computational-experimental investigation of the impact of novel ionic liquid electrolytes on performance characteristics, such as cycle life and dendrite growth/suppression, on Li metal electrodes in LMB. We have assembled a cross-cutting and cross-Center team of experts to tackle this problem. Computational studies, led by ARC, consisted of molecular dynamics simulations and *ab initio* computations to model several promising IL electrolytes such as [pyr14][TSFI] and [pyr13][FSI] [7]. Molecular dynamics (MD) simulations are atomic level modeling tools to investigate the structure, dynamics and thermodynamics as a function of temperature and voltage of large collections of molecules. During Phase I, two major computational tool development tasks were performed; a high fidelity "polarizable force field" (PFF) was implemented into our simulation codes and the capability to treat electrode/electrolyte interfaces under an

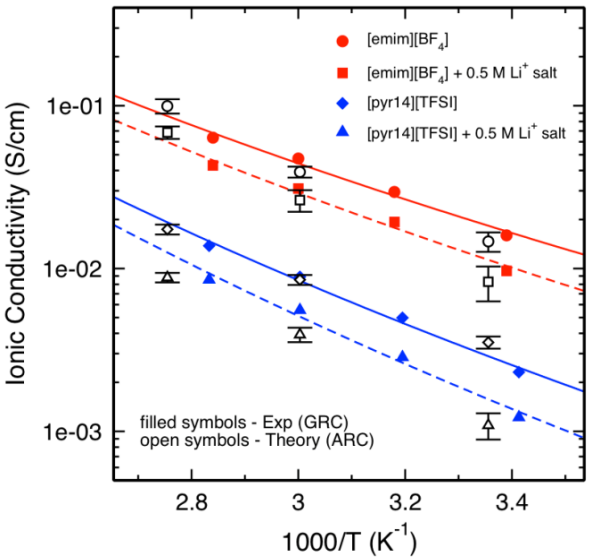

Figure 2 Ionic Conductivity

applied voltage was developed. These simulations were compared with experimental measurements to support the experimental electrolyte optimization and screening effort.

Ab initio methods are well-established quantum chemistry tools for accurately modeling reactive processes. During Phase I, these techniques were used to determine basic structural and electronic properties of the specific IL molecular species and also to identify interfacial chemical reactions without an applied voltage.

Phase I experimental studies, led by GRC, characterized fundamental properties of electrolytes including ionic conductivity to evaluate the performance of each electrolyte in laboratory LMBs. Electrolyte compatibility with electrode materials were performed via cyclic voltammetry (CV). CV helps identify the presence of undesirable decomposition reactions, as well as the required Li plating and stripping processes which are essential for a viable LMB. Electrochemical impedance spectroscopy (EIS) helped further characterize the performance of the electrolytes in LMBs. EIS scans, performed over the lifetime of a cell, identify sources of performance loss (loss of ionic conductivity, surface area development, and resistive film growth). After cycling, cell components were examined for evidence of morphology changes and visual evidence of decomposition of the electrolyte. Scanning electron microscopy (SEM) was used to characterize morphology changes, including dendritic growth, of the cycled electrodes. Optical microscopy was performed to visually characterize the nature of the electrode surface deposits. Energy dispersive X-ray spectroscopy (EDS) provided evidence of elemental compositions of the morphological features. This task revealed the physical changes of the Li electrodes after cycling, and identified possible decomposition products on the surface. These analyses helped explain why the cell did or did not perform as expected. Properties and performance were assessed and compared to the computational analysis results and traditional battery metrics.

Accomplishments

In Phase I, two different IL electrolytes were considered. First, [pyr14][TFSI] which has been shown to form a stable SEI layer which promotes stable cycling with Li metal, and non-trivial dendrite suppression in laboratory systems. Second, [EMIM][BF_4] forms a poor SEI layer and shows limited cycle stability with Li metal. In addition, literature studies with [EMIM][BF_4] have demonstrated short-circuiting due to dendrite growth in as little as 100 cycles. Our ultimate goal is to determine why one IL promotes stable cycling with dendrite suppression while the other does not. Understanding the suppression mechanism will lead to the design of new electrolytes that will ultimately solve this long-standing problem and will result in dramatic improvements in battery storage capacity.

Our Phase I project began by considering the properties of ILs as isolated systems. The molecular structures for isolated cation-anion pairs (gas phase) which are the basic units of ILs were determined by computational chemistry optimization (Phase I milestone (PIM)-C1). To assess their effectiveness as electrolytes, it was important to understand their structure, thermodynamics, transport properties and electrochemical stability. In MD simulations, the quality of the simulation depends critically on the quality of the force field used to evolve the system. Such simulations are particularly challenging for ILs due to the ability of the ions to polarize depending on the local environment. Including these effects accurately in simulations requires the use of a *"polarizable"* force field (PFF). Overwhelmingly, simulations in the literature do <u>*not*</u> use such PFFs, and therefore, their results are often largely qualitative. Recently, however, a very accurate PFF has been developed by one of our collaborators Dr. Oleg Borodin from the Army Research Lab [8]. The ARC computational group uses the state-of-the-art MD code from Sandia National Lab called LAMMPS. The first computational task for our Phase I project was to implement Borodin's PFF into LAMMPS. This implementation took more than a month of work and was not proposed in our Phase I proposal. However, the result is that we now have a robust predictive tool with the benefit of a highly accurate PFF together with the full capabilities of a general purpose simulation code.

In our first simulations, we evaluated the structure, thermodynamics and transport properties of the two ILs as a function of temperature and also of Li ion concentration (PIM-C2, PIM-C3). Detailed structural information of the ILs was obtained. Equilibrium thermodynamic quantities were also computed from the simulations including density, heat capacity, thermal expansion, etc. We also evaluated non-equilibrium properties such as diffusivity, ionic conductivity, and viscosity. Experimental measurements were conducted in parallel at GRC for diffusivity, ionic conductivity and viscosity (PIM-E1-E2). These properties have significant influence on rate capability of functioning cells. Laboratory data for neat ionic liquids matched closely with literature values [3]. Agreement between MD

simulations and experiments is very good for density, diffusion, ionic conductivity and viscosity. For the IL with the Li salt, the agreement is very good for density and viscosity and reasonable for diffusion and conductivity. This result demonstrates the effectiveness of the MD methods for forecasting properties of candidate electrolytes. Results for ionic conductivity are shown in Figure 2.

Next, we used MD simulations to investigate the properties of the ILs in the presence of an electrode surface (PIM-C4). For battery applications, it is important to understand the behavior of electrochemical interfaces under an applied voltage. Our MD simulation code LAMMPS, however, was not capable of simulating that situation. Therefore, we performed a second major upgrade of LAMMPS to include applied voltages. Implementation of this capability was a two month effort to perform and was not part of our original Phase I proposal which envisioned simulating interfaces at zero potential only. However, clearly it is a significant enhancement of our predictive modeling ability to treat the nonzero potential case. In addition to the software implementation, we also performed simulations of IL-graphite interfaces at a representative voltage (2.0 V). Under an applied voltage, charge accumulates on the electrode surface generating an electric field in the electrolyte. The electrolyte responds by forming a layer of opposite charge at the interface. This electric double layer (EDL) is fundamental in electrochemistry. In our simulations, we studied the formation, structure and properties of the EDL for our ILs. The MD simulations show molecular multi-level layering in the liquid: anions accumulate at the cathode and cations at the anode. Next, we consider chemical reactions between IL electrolytes and Li metal surfaces. Identifying which reactions occur and what products are produced is a critical step in understanding the factors that drive dendrite growth and subsequently in devising suppression strategies. To study interfacial chemistry, we performed *ab initio* MD simulations to investigate possible reactions at non-zero temperature (PIM-C5). We performed room temperature, *ab initio* MD simulations for Li slab with a thickness of seven atomic layers and with one ion of the IL ion pair on each side of the slab. Interestingly, we found for [EMIM][BF_4] that both ions remained bound to the surface without reacting. The situation was dramatically different for [pyr14][TFSI] where the cation stayed bound without reacting; however, the TFSI anion decomposed almost immediately and was effectively consumed by the Li surface. Before and after frames of the decomposition products are shown in Figure 3. The initial decomposition reaction was the loss of an F^- ion from the TFSI. The F^- was absorbed by the surface where it reacted again forming LiF as a product. Other atoms from the TSFI also reacted with the surface Li atoms to form other products including Li_2O.

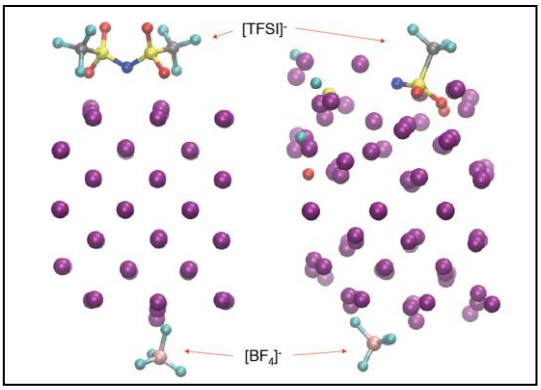

Figure 3 Simulation of anion decomposition on Li metal surface: before (left) and after (right).

To understand these mechanisms in more detail, we performed computational chemistry computations (PIM-C6). We considered 24 different mechanisms to remove F from BF_4 and TSFI. In all cases considered, we could not find an energetically favorable route to remove an F from BF_4. On the other hand, we found only in the presence of Li was it possible energetically to remove an F from TSFI. These computations are thus consistent with the simulations. Moreover, these computations may explain why [pyr14][TFSI] cycles stably without additives, whereas [EMIM][BF_4] does not. This also suggests that reaction energetics could be a powerful screening/design tool for IL electrolytes to predict important reaction products such as possibly LiF. Most electrochemical reactions however occur at non-zero voltage whereas the reactions studied during Phase I were all at zero voltage. In Phase II, we proposed to develop a novel and unique predictive tool to perform *ab initio* simulations with non-zero voltages. This will allow us study in detail how the character of interfacial reactions changes with voltage.

To complement the computational work performed for these two ionic liquids, a parallel experimental effort was performed at GRC to assess the electrochemical performance of each material. Coin cells were used as the standard test vehicle because they are easy to assemble and provide reproducible data that can be used to assess the performance of the ionic liquid in cell format. This effort focused on the use of symmetric coin cells utilizing two electrodes of lithium metal. The symmetric coin cell allows the ionic liquid to be tested directly with lithium metal as both the cathode and anode, removing the level of uncertainty which may arise with the use of a standard cathode material whose reactions and interactions with these ionic liquids may be unknown. Figure 4 illustrates the construction of a symmetric lithium metal coin cell.

The lithium metal electrodes used for these coin cells were 5/8-inch diameter discs of 0.005-inch thickness. The separator used was a Celgard M825, a 16µm tri-layer material commonly used in lithium ion cells.

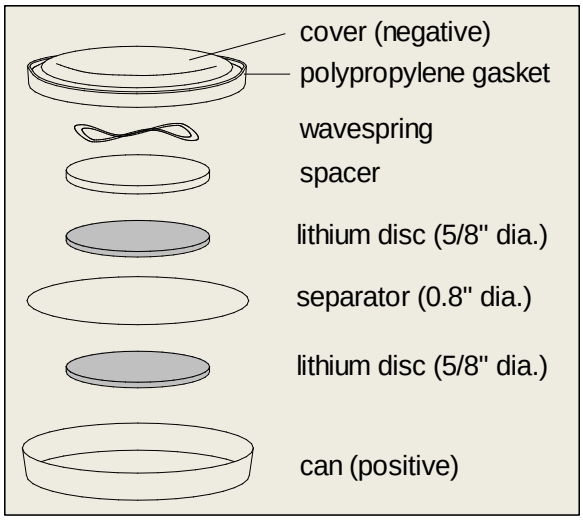

Figure 4 - Symmetric coin cell construction

Once the symmetric coin cells were constructed, cycling was performed at a controlled constant current of ±0.1mA/cm^2, with the area calculated based on the area of one lithium metal electrode, in a controlled 20°C environment. This current was consistent with similar work done in this area.[1] Cycling allows for the observation of the ability of the electrolyte to transfer Li efficiently without undesirable reactions in the presence of Li metal. Unless otherwise noted, these were the standard materials and conditions used in most coin cell experiments.

[pyr14][TFSI]

Several sets of coin cells were constructed containing the [pyr14][TFSI] ionic liquid electrolyte. Each cell was "flooded" with 30µL of electrolyte to ensure the coin cell contained a sufficient volume.

An initial set of two coin cells cycled with a 30-minute cycle regime, or 15-minute charges with 15-minute discharges and no rest periods. These cells were made with 0.030" thickness lithium metal as opposed to 0.005" lithium. These cells cycled for over 3000 cycles within a symmetric 30-minute voltage window as shown in Figure 5 indicating the cells remained healthy without dendrite growth causing short-circuiting.

An additional set of coin cells with [pyr14][TFSI] was made to assess the effects of the test regime on the performance of the cells. **Error! Reference source not found.**outlines the test regimes in this experiment.

Table 1 - Test regimes for [pyr14][TFSI] experiment IL-5

Cells	Charge (min)	Rest (min)	Discharge (min)
A,B,C,D	15	0	15
E,F	15	5	15
G,H	60	0	60

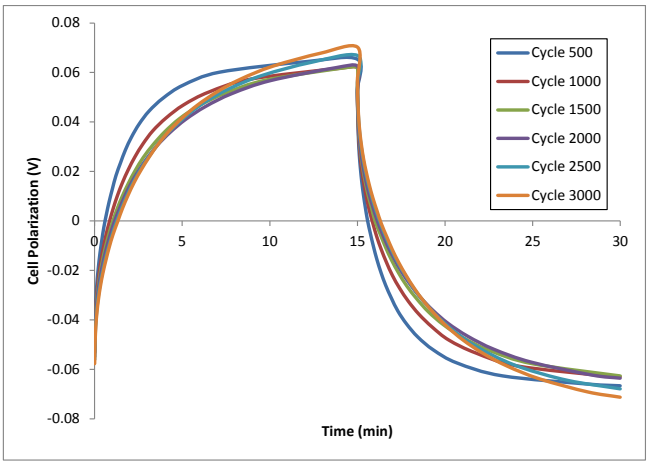

Figure 5 - [pyr14][TFSI] coin cell symmetric cycling with 30-mil Li metal

The 30-minute cycle was considered the baseline case against which the other regimes were compared. Figure 6 shows very symmetric cycling of a [pyr14] Li metal cell for over 1750 cycles, indicating the cell remained healthy and had not been short-circuited due to dendrite growth. It is assumed the difference in cycles accrued between this experiment and the original is due to the shift to using 0.015" thickness lithium metal.

The cell polarization decreased with increasing cycles, which agrees with electrochemical impedance trends observed for companion cells. Cells C and D underwent cycling under the same 30-minute cycle regime, but testing was paused incrementally to obtain electrochemical impedance data. Via electrochemical impedance spectroscopy, the impedance of the coin cells was measured at different intervals, including beginning of life, to quantify changes in resistance over time. The overall impedance of these cells decreased with cycling, consistent with increasing surface area of the Li metal electrodes as observed via microscopic analysis. This decreasing resistance trend can be seen on Figure 7, with the x and y axes in units of Ohms.

Of interest in these experiments was the effect of rest periods between half-cycles. To observe this effect, 5-minute rests were added between charge/discharge periods

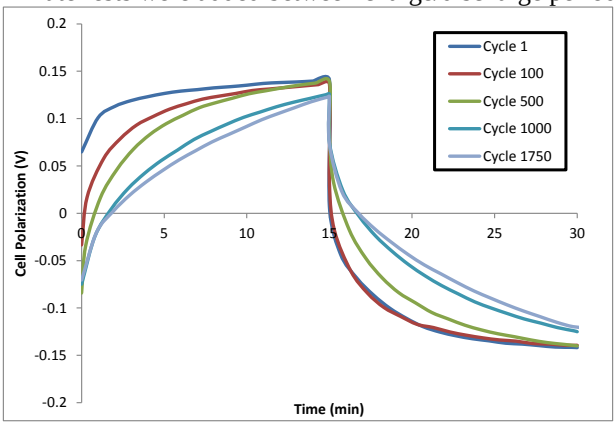

Figure 6 - [pyr14][TFSI] coin cell symmetric cycling

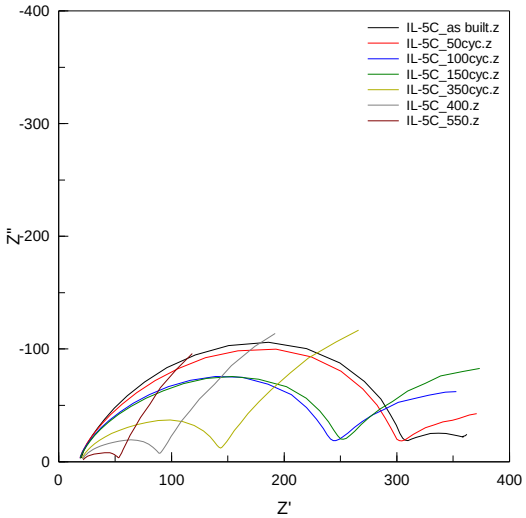

Figure 7 - Impedance spectra for [pyr14][TFSI] cells

in the 30-minute cycle regime, essentially increasing the total cycle time to 40 minutes. These cells cycled within a tighter voltage window, but the same trend of decreasing polarization with increasing cycles was observed (Figure 8).

Also of interest was the effect of longer cycle times on the lifetime and cycling characteristics of the cells. These cells were tested with a 2-hour cycle regime, or 60-minute charge/discharge periods, which represents a more realistic cycle period for real-world battery use. As Figure 9 depicts, these cells showed similar trends with symmetric cycling, but the polarization increased between cycles 100 and 500 and the cells failed after less than 700 cycles.

[EMIM][BF4]

Significantly more effort went into the cycling of [EMIM][BF4] ionic liquid because initial experiments produced coin cells with [EMIM][BF4] that would not cycle. It was determined through wetting experiments that [EMIM][BF4] was not successfully wetting the Celgard M825 separator. Without electrolyte filling the pores of the separator, the cell will not conduct ions and cannot cycle. In order to cycle [EMIM][BF4], different separators were investigated.

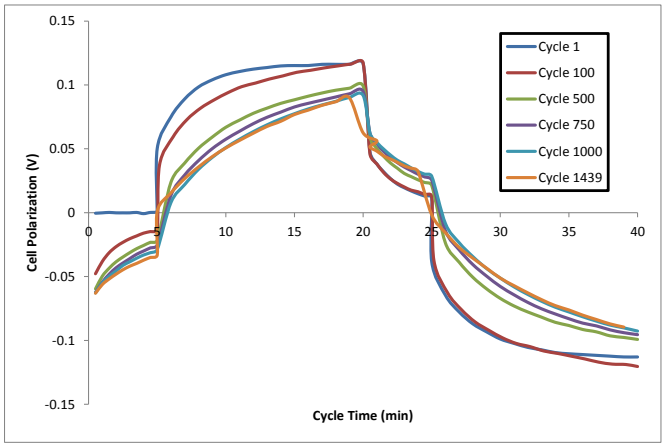

Figure 8 - [pyr14] symmetric cycling with rests

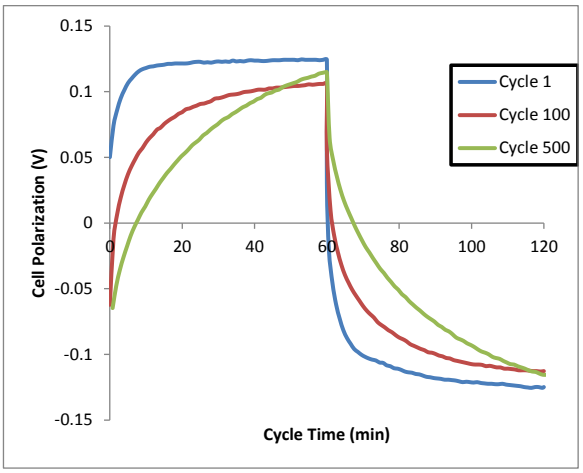

Figure 9 - [pyr14][TFSI] coin cells with 2-hour cycles

Since the selected separator did not cycle, two alternative separators were investigated – Hollingsworth & Vose (H&V) and glass fiber. Initial experimentation with both alternative separators showed little to no wetting at 20°C. By applying five drops of electrolyte to the separator and putting under vacuum for 8 hours at 60°C, the wettability improved. Once it was visually confirmed that the separator was wetted and additional drops of electrolyte were added to ensure the cell was "flooded", the coin cells were constructed and cycled for 20-minute cycles. Initially these coin cells showed low cell functionality and high cell impedance at 20°C. By increasing the test temperature to 60°C, the cells were able to cycle and a significant decrease in impedance was observed. The glass fiber separator coin cell cycled for only 20 cycles at 60°C before the cell polarized in one direction, so this separator was abandoned and focus shifted to the H&V separator.

The cell with H&V cycled for over 100 cycles at 60°C, but the cells continued to polarize as cycles accrued, which is the opposite trend witnessed with [pyr14][TFSI]. Figure 10 depicts this increase in polarization as the cell cycled. Resistance data supports the cycling data as it shows increasing resistance with cycling, consistent with the growth of a resistive film or decomposition of the electrolyte. Figure 11 depicts the large resistance of the cell at 20°C with an inset showing the smaller, yet increasing,

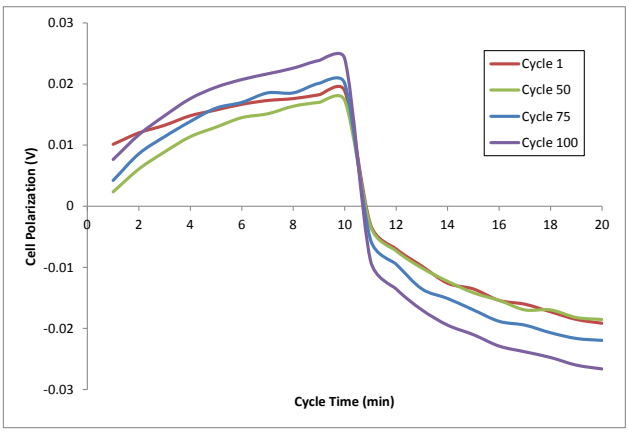

Figure 10 - [EMIM][BF4] coin cells with H&V Separator

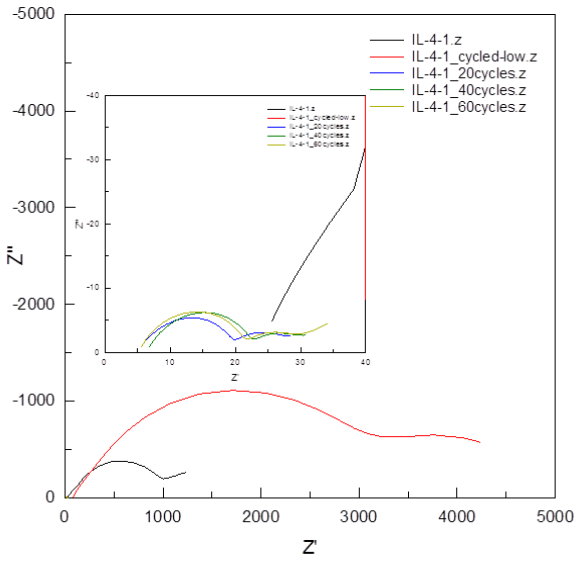

Figure 11 - Impedance spectra for [EMIM][BF4] with H&V Separator

resistance at 60°C. On this figure, the black and red lines represent data collected at 20°C while the blue, light and dark green were collected at 60°C and are so small in comparison with 20°C that they cannot be seen on the 20°C scale. Figure 12 compares the increase in internal resistance as cells with [EMIM][BF4] are cycled with the decrease in internal resistance as cells with [pyr14][TFSI] are cycled.

It was hypothesized that the wetting issues and poor functionality may be due to impurities in the [EMIM][BF4], so a purer "electrochemical grade" was obtained and tested (>99% versus >98%). Wetting experiments were repeated with H&V and both Celgard separators. Again, the separators were soaked at 60°C overnight and all were visibly wet before constructing the cells. Performance with either Celgard separator remained poor as neither cycled at 20°C and produced only limited cycles at 60°C. However, performance improved slightly against the H&V separator. Cells containing "electrochemical grade" [EMIM][BF4] cycled for roughly 150 cycles, slightly higher than the lower purity material, before polarizing in the negative voltage direction, possibly

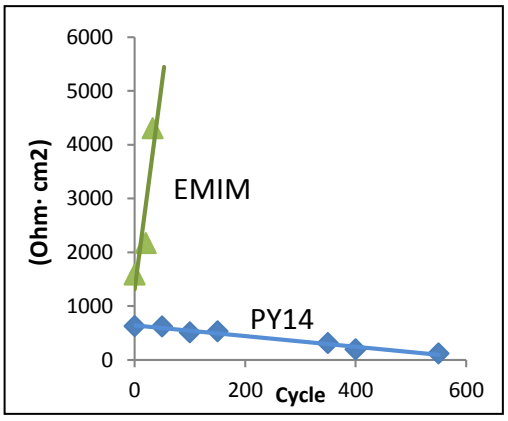

Figure 12 - Charge transfer resistance in coin cells

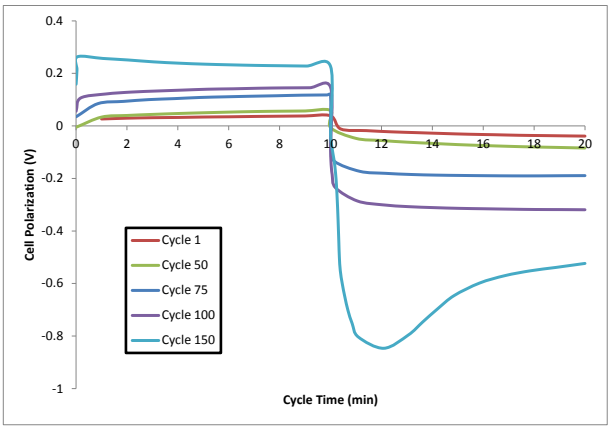

Figure 13 - [EMIM][BF4] Electrochemical grade coin cell with H&V separator

due to lithium plating on one electrode and failing to strip back upon discharge (see Figure 13). Overall, the "electrochemical grade" ionic liquid did not have a significant impact on the performance in coin cells.

Voltage polarization and increasing internal resistance are consistent with growth of a resistive film. These trends were corroborated by visual inspection SEM observations. These revealed a change in the color and consistency of [EMIM][BF4] after it had been cycled with Li metal. [EMIM] [BF4] became partially solidified with a concentrated amber color deposited onto the Li metal surface. The increase in impedance of [EMIM] [BF4] could also be due to decomposition of the electrolyte as the cell was cycled, which would also explain the limited number of cycles [EMIM][BF4] achieved. Such decomposition of [EMIM][BF4] is also consistent with the results of cyclic voltammetry experiments.

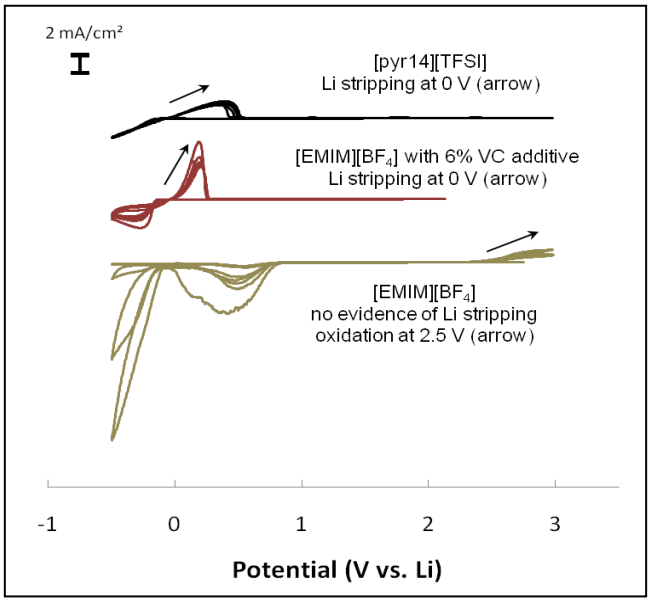

Figure 14 Cyclic voltammetry shows Li plating and stripping for [pyr14][TSFI]. [EMIM][BF4] requires VC additive to suppress decomposition.

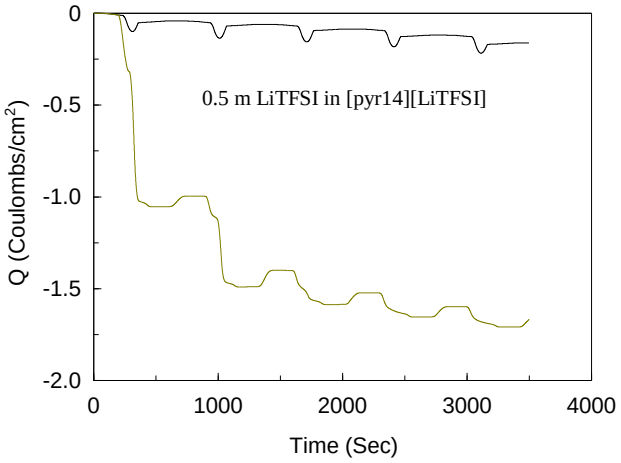

Figure 15 Cycling efficiency of [pyr14][TSFI]-based electrolyte and [EMIM][BF4]-based electrolytes.

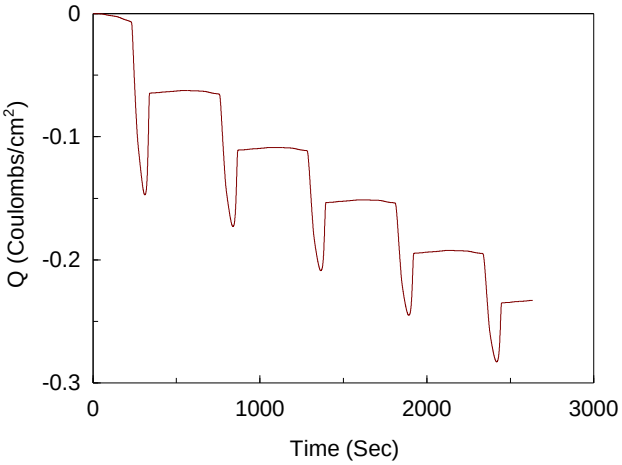

Figure 16 Enhancement of cycling efficiency of [EMIM][BF4]-based electrolyte with 6% VC additive.

Cyclic voltammetry (CV) experiments on nickel electrodes produced clues to explain the differences in cycling with Li metal. Data for [EMIM][BF4] showed significant decomposition reactions as the electrode was driven to the potential seen at a Li electrode, with little capability for cycling (plating and stripping of Li metal). Addition of 6% VC additive improved cycling of [EMIM][BF4], and we intend to use this additive in Phase II to study its effect on improved cycling capabilities of selected high performance electrolytes. Potential stability of [pyr14][TSFI] is significantly better than [EMIM][BF4]. In this testing, [pyr14][TSFI]- showed evidence of Li plating and stripping around 0.0 V vs. Li, with suppression of decomposition in repeated cycling: elements essential for cycling with Li metal. These differences were expected and formed the basis for selecting these materials for study. Cyclic voltammograms for these electrolytes are contrasted in Figure 14.

Cycling efficiency information was extracted from the voltammetry data in Figure 14, by integrating current with respect to time, over five successive cycles. This analysis shows that electrolyte based on [pyr14][TSFI] develops a lithium cycling efficiency of 79% in the second cycle. In contrast, the only charge accumulation processes for [EMIM][BF_4]-based electrolytes correspond to electrolyte decomposition, with a cycling efficiency of essentially 0%. Capacity versus time for these electrolytes is contrasted in Figure 15. Addition of 6% VC to [EMIM][BF_4]-based electrolyte, dramatically improved lithium cycling capability, achieving an efficiency of approximately 50% (see Figure 16).

Our computational modeling has provided reasons for some of these electrochemical differences, showing that [pyr14][TSFI] reacts with Li and forms a protective layer, while the [EMIM][BF_4] does not. Refinement of the computational tools developed in this work could be used to predict optimized electrolytes which further promote the formation of stable SEI layers for a variety of electrolytes.

Additive chemistries could similarly be explored computationally.

Li electrodes were harvested from cycled cells and examined by SEM and EDS, to observe physical changes of the Li electrodes after cycling, and identify possible decomposition products on the surface. Optical microscopy was also performed to visually characterize the nature of the electrode surface deposits. Results showed the formation of thick waxy films on the surface of Li metal, when cycled with [EMIM][BF_4]-based electrolytes. Elemental mapping shows heavy concentrations of carbon and fluorine in the region of the films, supporting that the films have been formed by electrolyte decomposition. Cycling was limited to ~130 cycles with this electrolyte, and little evidence of dendrite growth is observed.

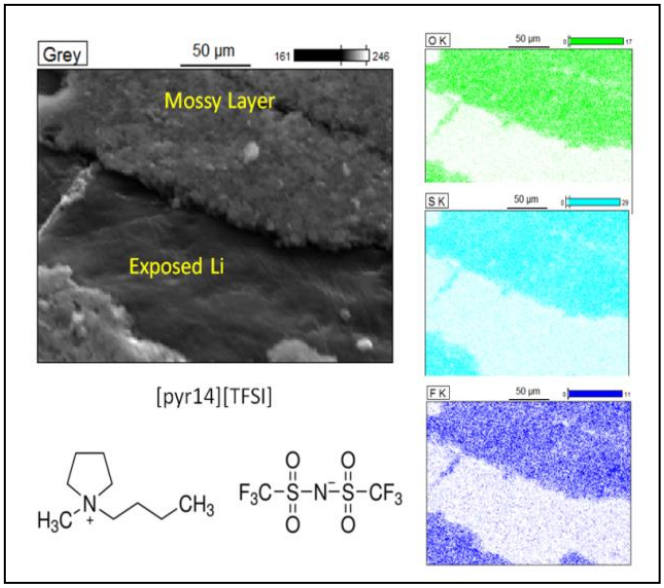

Figure 17 SEM image of Li surface. Analysis shows O, S and F concentrated in mossy layers.

Analysis of the Li cycled 2000 cycles, with [pyr14][TSFI]-based electrolyte, reveals a compacted mossy layer of Li, which is not strongly bound to the metallic Li underneath. EDS analysis revealed elements associated with the electrolyte (O, C, S, and F) concentrated in regions where the mossy layer was present. This observation is consistent with the formation of an SEI layer on the large surface area of the mossy Li. Regions where the mossy layer was removed revealed a textured Li surface. The high surface area of the mossy layer explains the reduced impedance with cycling in [pyr14][TSFI]-based electrolyte.

Conclusions

In this Phase I Seedling project, Lithium metal batteries (LMB)s with two different IL electrolytes were considered: [pyr14][TSFI] [4] which has shown significant dendrite suppression and Li anode cycling ability on the order of 1000 cycles in laboratory systems and [EMIM][BF_4] [5] which has shown little or no dendrite suppression and very poor cycle life [6]. For these two cases, we performed the following studies. First, we determined properties of isolated ILs important for battery operation such as density, conductivity, diffusivity, viscosity, etc. Good agreement between simulation and experiment was found. Second, we made predictions about the structure and properties of the IL in the presence of an electrode; interaction of the ILs with the anode surface affects the local molecular ordering of the IL as well as its properties. Third, we considered chemical reactions between the IL electrolyte and the Li metal anode surface at zero applied voltage using computational chemistry. Rapid decomposition of the TFSI anion was observed on the Li surface while other species remained relatively stable. Finally, we built and characterized the performance of laboratory LMBs using the two ILs. A comprehensive experimental characterization was performed indicating that fundamentally different surface layers were formed on the Li electrodes depending on the electrolyte. These differing surfaces layers were ultimately responsible for the dramatically different cycling performance. Strong correlations were found between computations and experimental battery characterizations.

Phase I Milestones

All Phase I computational milestones were completed:

C1) *Ab initio* computations of IL molecular species
C2) MD simulations of pure IL structure, thermodynamics and diffusivity
C3) MD simulations of ILs doped with Li+ ions for solvation and ionic conductivity
C4) MD simulations of IL, Li metal interface to determine interfacial properties
C5) *Ab initio* simulations of initial interface reaction mechanisms and products
C6) *Ab initio* computations of surface reaction barriers

All Phase I experimental milestones were completed:

E1) IL diffusivity measurements
E2) IL ionic conductivity measurement
E3) IL potential stability measurement
E4) Cycling efficiency of Li metal cell evaluated
E5) Electrochemical impedance of Li electrode during/after cycling evaluated
E6) SEM/EDS to evaluate electrode surface changes with cycling

Current TRL: 2-3

Applicable NASA Programs/Projects

Several programs in ARMD and OCT could benefit from our Seedling project. We had preliminary contact with program managers but we will have more intensive discussions after we have obtained a complete set of results. Advanced Li metal anode battery technology has the potential to enable future electric aircraft and also contribute to many other NASA applications requiring safe, highly efficient, energy storage.

Publications and Patent Applications

3-4 journal publications are expected from this project

References

1 Galinski et al, Electrochimica Acta 51 (2006) 5567-5580
2 NASA/CR–2011-216847, Subsonic Ultra Green Aircraft Research: Phase I Final Report
3 Schweikert et al, J. Power Sources 228 (2013) 237-243
4 [pyr14][TFSI] = 1-butyl-1-methylpyrrolidinium bis(fluoro-sulfonyl)imide
5 [EMIM][BF4] = 1-ethyl-3-methyl imidazolium tetrafluoroborate
6 Bhattacharyya et al, Nature Mat. 9, (2010) p 504
7 Borodin et al, J. Phys. Chem .B 110, (2006) p 16879
8 [pyr13][FSI] = 1-propyl-1-methylpyrrolidinium bis(trifluoro-methanesulfonyl)imide